Scientific Research and Essay Vol.4 (3), pp. 131-140, March, 2009
Available online at http://www.academicjournals.org/SRE
ISSN 1992-2248 © 2009 Academic Journals

Full Length Research Paper

Deformations and stresses in rotating FGM pressurized thick hollow cylinder under thermal load

M. Zamani Nejad and G. H. Rahimi*

Mechanical Engineering Department, Tarbiat Modares University, Tehran, Iran.

Accepted 13 January, 2009

Using the infinitesimal theory of elasticity, closed form solutions for one-dimensional steady-state thermal stresses in a rotating functionally graded (FGM) pressurized thick-walled hollow circular cylinder are obtained under generalized plane strain and plane stress assumptions, respectively. The material properties are assumed to vary nonlinearly in the radial direction and the Poisson's ratio is assumed constant. The temperature distribution is assumed to be a function of radius, with general thermal and mechanical boundary conditions on the inside and outside surfaces of the cylinder. The direct method is used to solve the heat conduction and Navier equations. The steady-state temperature, displacements and stresses distributions depending on an inhomogeneity constant are compared with those of the homogeneous case and presented in the form of graphs. The values used in this study are arbitrary chosen to demonstrate the effect of inhomogeneity on displacements, and stresses distributions.

Key words: FGM, hollow circular cylinder, rotating, thermal stresses, elasticity.

INTRODUCTION

The research on the prediction of stresses in rotating thick hollow cylinder has never ceased because of the importance of these basic structures in numerous mechanical, civil, electrical and computer engineering applications. Plane strain and plane stress analytical solutions of thick hollow cylinder problems in the elastic stress state have been available for many years in standard and advanced textbooks (Rees, 2000; Timoshenko and Goodier, 1970; Ugural and Fenster, 2003). Recently, a new class of composite materials known as functionally graded materials (FGMs) has drawn considerable attention. FGMs are composite materials that are microscopically inhomogeneous and the mechanical properties vary smoothly or continuously from one surface to another. Typically, these materials are made from a mixture of ceramic and metal or a combination of different materials. Due to their excellent features, FGMs are finding increasing applications in many engineering sectors (Noda, 1991; Tanigawa, 1995) especially for working in high temperature environments where thermal effects due to temperature change must be taken into account. Obata and Noda (1994) through the application of a perturbation approach, investigated the thermal stresses in an FGM hollow sphere and in a hollow circular cylinder. The aim of researchers is to understand the effect of composition on stresses and to design the optimum FGM hollow circular cylinder and hollow sphere. A work was also published by Horgan and Chan (1999) where it was noted that increasing the positive exponent of the radial coordinate provided a stress shielding effect whereas decreasing it created stress amplification. Assuming that the material has a graded modulus of elasticity, while the Poisson's ratio is a constant, Tutuncu and Ozturk (2001) investigated the stress distribution in the axisymmetric structures. They obtained the closed-form solutions for stresses and displacements in functionally graded cylindrical and spherical vessels under internal pressure. Based on approximate solutions of temperatures and thermal stresses, the optimization of the material composition of FGM hollow circular cylinders under thermal loading was discussed (Ootao et al., 1999). Applying the Frobenius series method, Zimmerman and Lutz (1999)

*Corresponding author: E-mail: rahimi_gh@irost.org. or mzamani@modares.ac.ir. Tel.: +98-2188826830. Fax: +98-2188838328.

found a way round the problem of the uniform heating of functionally graded circular cylinder. They derived the exact solution for the problem of radially heated cylinder whose modulus of elasticity and thermal expansion coefficient vary linearly with radius. Another general analysis of one-dimensional steady-state thermal stresses in a hollow thick cylinder made of functionally graded material was obtained (Jabbari et al., 2002). In addition, an analysis of the thermo-mechanical behavior of hollow circular cylinders of functionally graded materials was presented (Liew et al., 2003). They worked out a solution based on the solutions obtained by a novel limiting process that makes use of the solutions of homogeneous hollow circular cylinders, without resorting to the basic theory or the equations of non-homogeneous thermoelasticity. Tarn and Wang (2004) studied heat conduction in circular cylinders of functionally graded materials and laminated composites. They focused on the end effects and by means of matrix algebra and eigen function expansion, the decay length that characterizes the end effects on the thermal filed was assessed. In an attempt to derive the series solutions of temperature, displacements and thermal/mechanical stresses in a functionally graded circular hollow cylinder, assuming that the material properties are temperature-independent and radially dependent, but homogeneous in each layer, Shao (2005) used a multi-layered approach. The theoretical basis was taken to be the theory of laminated composites. Pan and Roy (2006) derived exact solutions for multilayered FGM cylinders under static deformation. They obtained these solutions by making use of the method of separation of variables and expressed it in terms of the summation of the Fourier series in the circumferential direction. Jabbari et al. (2007), making use of the generalized Bessel function and Fourier series solved the temperature and Navier equations analytically and offered a general theoretical analysis of three-dimensional mechanical and thermal stresses for a short hollow cylinder made of functionnally graded material. In a study carried out by You et al. (2007), the deformations and stresses in thick-walled cylindrical vessels made of functionally graded materials were obtained. Such vessels have a varying Young's modulus and thermal expansion coefficient and are subjected to internal pressure and uniform temperature change. Given the assumption that the material is isotropic with constant Poisson's ratio and exponentially varying modulus of elasticity through the thickness, Tutuncu (2007) obtained power series solutions for stresses and displacements in functionally-graded cylindrical vessels subjected to internal pressure alone. Argeso and Eraslan (2008), assuming the different states of material properties including Poisson's ratio, modulus of elasticity, the yield strength, the coefficient of thermal expansion and thermal conductivity, assessed the thermo-elastic response of cylinders and tubes. In a recent study by Chen and Lin (2008), assuming that the property of FGMs is in exponential function form, they conducted the elastic analyses for both a thick cylinder and a spherical pressure vessel which were made of func-tionally graded materials. Assuming that thermo-mecha-nical properties of functionally graded materials are temperature independent and vary continuously in the radial direction of the cylinder. Shao and Ma (2008) by making use of Laplace transform techniques and series solving method for ordinary differential equation, obtained solutions for the time-dependent temperature and unsteady thermo-mechanical stresses in functionally graded circular hollow cylinder.

MATERIALS AND METHODS

Consider a thick-walled FGM cylinder with an inner radius a, and an outer radius b, subjected to internal and external pressures P_i and P_o that are axisymmetric and rotating at a constant angular speed ω about its axis. The cylindrical coordinates (r, θ, z) are considered along the radial, hoop and axial directions, respectively. The deformations and stresses in the thick-walled cylinder are symmetric. The stress equilibrium equation can be written as:

$$\frac{d}{dr}(r\sigma_{rr}) - \sigma_{\theta\theta} = -\rho r^2 \omega^2 \tag{1}$$

Where σ_{rr} and $\sigma_{\theta\theta}$ are the radial and hoop stress components, respectively; ρ is density.

For the thick hollow cylinder, σ_{rr} and $\sigma_{\theta\theta}$ are given in terms of the displacement u_r by

$$\sigma_{rr} = (A_{11}\frac{du_r}{dr} + A_{12}\frac{u_r}{r} + A_{13}\alpha T)E \tag{2}$$

$$\sigma_{\theta\theta} = (A_{12}\frac{du_r}{dr} + A_{11}\frac{u_r}{r} + A_{13}\alpha T)E \tag{3}$$

where $E(r)$ is modulus of elasticity and A_{11}, A_{12}, and A_{13} are related to Poisson's ratio υ as:

Plane strain condition:

$$A_{11} = \frac{1-\upsilon}{(1+\upsilon)(1-2\upsilon)}$$
$$A_{12} = \frac{\upsilon}{(1+\upsilon)(1-2\upsilon)}$$
$$A_{13} = -\frac{1}{1-2\upsilon} \tag{4}$$

Plane stress condition:

$$A_{11} = \frac{1}{1-\upsilon^2}$$
$$A_{12} = \frac{\upsilon}{1-\upsilon^2}$$
$$A_{13} = -\frac{1}{1-\upsilon} \tag{5}$$

The substitution of equations (2) and (3) into equation (1) produces the Navier equation

$$\frac{d^2u_r}{dr^2}+(\frac{1}{E}\frac{dE}{dr}+\frac{1}{r})\frac{du_r}{dr}+(\frac{n}{Er}\frac{dE}{dr}-\frac{1}{r^2})u_r=-\frac{A_{13}}{A_{11}E}\frac{d(E\alpha T)}{dr}-\frac{\rho r\omega^2}{A_{11}E} \quad (6)$$

Where

$$n = \frac{A_{12}}{A_{11}}$$

Solution derived for FGM state

The material properties are assumed to be radially dependent. Given that the radial coordinate r is normalized as $\bar{r}=r/a$, the modulus of elasticity E, density ρ, linear expansion coefficient α and thermal conductivity k through the wall thickness are assumed to vary as follows;

$$E(r)=E_i(\bar{r})^{\beta} \quad (7.1)$$

$$\rho(r)=\rho_i(\bar{r})^{\mu} \quad (7.2)$$

$$\alpha(r)=\alpha_i(\bar{r})^{\eta} \quad (7.3)$$

$$k(r)=k_i(\bar{r})^{\xi} \quad (7.4)$$

Here E_i, ρ_i, α_i and k_i are the modulus of elasticity, density, linear expansion coefficient and thermal conductivity at the inner surface $r=a$ and β, μ, η and ξ are the in-homogeneity constants determined empirically. Since the variation of Poisson's ratio, υ for engineering materials is small, it is assumed constant. In the steady state case, the heat conduction equation for the one-dimensional problem in polar coordinates simplifies to;

$$\frac{\partial}{\partial r}(kr\frac{\partial T}{\partial r})=0 \quad (8)$$

The thermal boundary condition for an FGM hollow cylinder is given as;

$$k\frac{dT}{dr}=h_a(T-T_a) \quad \text{on} \quad r=a$$
$$-k\frac{dT}{dr}=h_b(T-T_b) \quad \text{on} \quad r=b \quad (9)$$

where T_a and T_b are the temperatures of the surrounding media, h_a and h_b are the heat transfer coefficients, and subscripts a and b correspond to surfaces $r=a$ and $r=b$, respectively. The general solution of equation (8) with considering relation of thermal transfer coefficient, equation (7.4) and boundary conditions, equation (9) is;

$$T=A_1(\bar{r})^{-\xi}+A_2 \quad (10)$$

where

$$A_1=\frac{\xi^{-1}(T_a-T_b)}{k_i(\frac{1}{ah_a}+\frac{1}{bh_b})+\xi^{-1}(1-a^{\xi}b^{-\xi})}$$

$$A_2=\frac{\frac{k_i}{ah_a}(T_a+T_b)+k_iT_a(\frac{1}{bh_b}-\frac{1}{ah_a})}{k_i(\frac{1}{ah_a}+\frac{1}{bh_b})+\xi^{-1}(1-a^{\xi}b^{-\xi})}+\frac{\xi^{-1}(T_b-a^{\xi}b^{-\xi}T_a)}{k_i(\frac{1}{ah_a}+\frac{1}{bh_b})+\xi^{-1}(1-a^{\xi}b^{-\xi})} \quad (11)$$

By substituting equation (10) into equation (6), the Navier equation would be;

$$r^2\frac{d^2u_r}{dr^2}+(\beta+1)r\frac{du_r}{dr}+(n\beta-1)u_r=B_1r^{\eta-\xi+1}+B_2r^{\eta+1}+B_3r^{\mu-\beta+3} \quad (12)$$

Where

$$B_1=-(\frac{A_{13}}{A_{11}})\frac{\alpha_iA_1(\beta+\eta-\xi)}{a^{\eta-\xi}}$$

$$B_2=-(\frac{A_{13}}{A_{11}})\frac{\alpha_iA_2(\beta+\eta)}{a^{\eta}}$$

$$B_3=-\frac{\rho_ia^{\beta-\mu}\omega^2}{A_{11}E_i} \quad (13)$$

Equation (12) is the non-homogeneous Euler differential equation with general and particular solutions whose complete solution u_r is;

$$u_r=C_1r^{m_1}+C_2r^{m_2}+C_3r^{m_3}+C_4r^{m_4}+C_5r^{m_5} \quad (14)$$

where m_1 to m_5 and C_3 to C_5 are as follows;

$$m_1 = \frac{-\beta + \sqrt{\beta^2 - 4n\beta + 4}}{2}$$
$$m_2 = \frac{-\beta - \sqrt{\beta^2 - 4n\beta + 4}}{2}$$
$$m_3 = \mu - \beta + 5$$
$$m_4 = \eta - \xi + 3$$
$$m_5 = \eta + 3$$
$$C_3 = \frac{B_3}{(\mu - \beta - m_1 + 5)(\mu - \beta - m_2 + 5)}$$
$$C_4 = \frac{B_1}{(\eta - \xi - m_1 + 3)(\eta - \xi - m_2 + 3)}$$
$$C_5 = \frac{B_2}{(\eta - m_1 + 3)(\eta - m_2 + 3)} \quad (15)$$

By substituting equation (14) into equations (2) and (3), the resulting stress expressions are;

$$\sigma_{rr} = C_1 E_i a^{m_1 - 1}(A_{11} m_1 + A_{12})(\bar{r})^{-m_2 - 1}$$
$$+ C_2 E_i a^{m_2 - 1}(A_{11} m_2 + A_{12})(\bar{r})^{-m_1 - 1}$$
$$+ C_3 E_i a^{m_3 - 1}(A_{11} m_3 + A_{12})(\bar{r})^{-m_1 - m_2 + m_3 - 1}$$
$$+ C_4 E_i a^{m_4 - 1}(A_{11} m_4 + A_{12})(\bar{r})^{-m_1 - m_2 + m_4 - 1}$$
$$+ C_5 E_i a^{m_5 - 1}(A_{11} m_5 + A_{12})(\bar{r})^{-m_1 - m_2 + m_5 - 1}$$
$$+ A_{13} A_1 E_i \alpha_i (\bar{r})^{-m_1 - m_2 + m_4 - 3}$$
$$+ A_{13} A_2 E_i \alpha_i (\bar{r})^{-m_1 - m_2 + m_5 - 3} \quad (16)$$

$$\sigma_{\theta\theta} = C_1 E_i a^{m_1 - 1}(A_{11} + A_{12} m_1)(\bar{r})^{-m_2 - 1}$$
$$+ C_2 E_i a^{m_2 - 1}(A_{11} + A_{12} m_2)(\bar{r})^{-m_1 - 1}$$
$$+ C_3 E_i a^{m_3 - 1}(A_{11} + A_{12} m_3)(\bar{r})^{-m_1 - m_2 + m_3 - 1}$$
$$+ C_4 E_i a^{m_4 - 1}(A_{11} + A_{12} m_4)(\bar{r})^{-m_1 - m_2 + m_4 - 1}$$
$$+ C_5 E_i a^{m_5 - 1}(A_{11} + A_{12} m_5)(\bar{r})^{-m_1 - m_2 + m_5 - 1}$$
$$+ A_{13} A_1 E_i \alpha_i (\bar{r})^{-m_1 - m_2 + m_4 - 3}$$
$$+ A_{13} A_2 E_i \alpha_i (\bar{r})^{-m_1 - m_2 + m_5 - 3} \quad (17)$$

For the hollow cylinder submitted to uniform pressures P_i and P_o on the inner and outer surfaces, respectively, the mechanical boundary conditions can be expressed as;

$$\sigma_{rr}\Big|_{\bar{r}=1} = -P_i \text{ ,} \qquad \sigma_{rr}\Big|_{\bar{r}=b/a} = -P_o \quad (18)$$

Substituting the boundary conditions (18) into equation (16), the constants of integration become;

$$C_1 = \frac{D_4 D_5 - D_2 D_6}{D_1 D_4 - D_2 D_3}$$
$$C_2 = \frac{D_1 D_6 - D_3 D_5}{D_1 D_4 - D_2 D_3} \quad (19)$$

where

$$D_1 a^{1-m_1} = D_3 b^{1-m_1} = A_{11} m_1 + A_{12}$$
$$D_2 a^{1-m_2} = D_4 b^{1-m_2} = A_{11} m_2 + A_{12}$$
$$D_5 = -C_3(A_{11} m_3 + A_{12}) a^{m_3 - 1}$$
$$- C_4(A_{11} m_4 + A_{12}) a^{m_4 - 1}$$
$$- C_5(A_{11} m_5 + A_{12}) a^{m_5 - 1}$$
$$- A_{13}\alpha_i(A_1 + A_2) - P_i / E_i$$
$$D_6 = -C_3(A_{11} m_3 + A_{12}) b^{m_3 - 1}$$
$$- C_4(A_{11} m_4 + A_{12}) b^{m_4 - 1}$$
$$- C_5(A_{11} m_5 + A_{12}) b^{m_5 - 1}$$
$$- A_{13}\alpha_i[A_1 (b/a)^{m_4 - 3}$$
$$+ A_2 (b/a)^{m_5 - 3}]$$
$$- (P_o / E_i)(b/a)^{m_1 + m_2} \quad (20)$$

Solution derived for homogeneous STATE

The material properties are

$$E^H = E_i \quad (21.1)$$
$$\rho^H = \rho_i \quad (21.2)$$
$$\alpha^H = \alpha_i \quad (21.3)$$
$$k^H = k_i \quad (21.4)$$

where superscript “H” represents the homogeneous state. The general solution of equation (8) with considering relation of thermal transfer coefficient equation (21.4) and boundary conditions (9) is;

$$T^H = A_1' \ln \bar{r} + A_2' \quad (22)$$

Where

$$A_1' = \frac{T_b - T_a}{k_i\left(\frac{1}{a h_a} + \frac{1}{b h_b}\right) + \ln\left(\frac{b}{a}\right)}$$
$$A_2' = \frac{k_i\left(\frac{T_b}{a h_a} + \frac{T_a}{b h_b}\right) + T_a \ln\left(\frac{b}{a}\right)}{k_i\left(\frac{1}{a h_a} + \frac{1}{b h_b}\right) + \ln\left(\frac{b}{a}\right)} \quad (23)$$

By substituting equations (21) and (22) into equation (6), the Navier equation would be;

$$r^2\frac{d^2u_r^H}{dr^2}+r\frac{du_r^H}{dr}-u_r^H = -\frac{A_{13}A_1'\alpha_i}{A_{11}}r-\frac{\rho_i\omega^2}{A_{11}E_i}r^3 \quad (24)$$

The complete solution for the above equation is;

$$u_r^H = C_1'r+C_2'r^{-1}+C_3'r^3+C_4'r^5 \quad (25)$$

Where

$$C_3' = -\frac{A_{13}A_1'\alpha_i}{8A_{11}}$$
$$C_4' = -\frac{\rho_i\omega^2}{24A_{11}E_i} \quad (26)$$

By substituting the equation (25) into the equations (2) and (3), the steady-state thermal stresses expression for the rotating homogeneous pressurized thick hollow cylinder are;

$$\sigma_{rr}^H = C_1'E_i(A_{11}+A_{12}) + C_2'E_i(-A_{11}+A_{12})a^{-2}(\bar{r})^{-2} + C_3'E_i(3A_{11}+A_{12})a^2(\bar{r})^2 + C_4'E_i(5A_{11}+A_{12})a^4(\bar{r})^4 + A_{13}A_1'E_i\alpha_i\ln\bar{r}+A_{13}A_2'E_i\alpha_i \quad (27)$$

$$\sigma_{\theta\theta}^H = C_1'E_i(A_{11}+A_{12}) + C_2'E_i(A_{11}-A_{12})a^{-2}(\bar{r})^{-2} + C_3'E_i(A_{11}+3A_{12})a^2(\bar{r})^2 + C_4'E_i(A_{11}+5A_{12})a^4(\bar{r})^4 + A_{13}A_1'E_i\alpha_i\ln\bar{r}+A_{13}A_2'E_i\alpha_i \quad (28)$$

The constants C_1' and C_2' are determined from the boundary conditions (equation 18) as;

$$C_1' = \frac{D_4'D_5'-D_2'D_6'}{D_1'D_4'-D_2'D_3'}$$
$$C_2' = \frac{D_1'D_6'-D_3'D_5'}{D_1'D_4'-D_2'D_3'} \quad (29)$$

Where

$$D_1' = D_3' = A_{11}+A_{12}$$
$$D_2'a^2 = D_4'b^2 = -A_{11}+A_{12}$$
$$D_5' = -C_3'(3A_{11}+A_{12})a^2 - C_4'(5A_{11}+A_{12})a^4 - A_{13}A_2'\alpha_i - P_i/E_i$$
$$D_6' = -C_3'(3A_{11}+A_{12})b^2 - C_4'(5A_{11}+A_{12})b^4 - A_{13}A_1'\alpha_i\ln(b/a) - A_{13}A_2'\alpha_i - P_o/E_i \quad (30)$$

RESULTS AND DISCUSSION

The analytical solution obtained in this paper may be checked for two examples. In the first example, the angular speed of the cylinder is considered constant and the power law index is considered variable. In the second example, the angular speed is considered variable and the power law index constant.

Example 1: Consider a hollow functionally graded cylinder of inner radius $a=0.5m$ and the outer radius $b=0.7m$, which is rotating around the $z-axis$ at the constant angular speed of $\omega=50rad/\sec$. A special case is considered in which there is no heat transfer taking place between the inner and outer surfaces with the surrounding medium $(h_a,h_b\to\infty)$ and the surface temperature at the inner and outer surfaces are prescribed as T_a and T_b, respectively. The boundary conditions for temperature are taken as $T_a=10^oC$, $T_b=0^oC$. The modulus of elasticity, density and thermal coefficient of expansion at the inner radius have the values of $E_i=200GPa$, $\rho_i=7860kg/m^3$, $\alpha_i=12(10^{-6})/^oC$, respectively. It is also assumed that the Poisson's ratio υ, has a constant value of 0.3. The applied internal and external pressures are $80MPa$ and $10MPa$ respectively. In addition, $\beta=\mu=\eta=\xi$ and β ranges from -3 to 3. The range $-3\le\beta\le3$ to be used in the pre-sent study covers all the values of coordinate exponent encountered in the references cited earlier.

For different values of β, module of elasticity, temperature profile, radial displacement, radial stresses, hoop stresses and the von Mises' equivalent stresses along the radial direction are plotted for plane strain and plane stress conditions in Figures 1–10.

It is apparent from the curve of Figure 1 that a positive

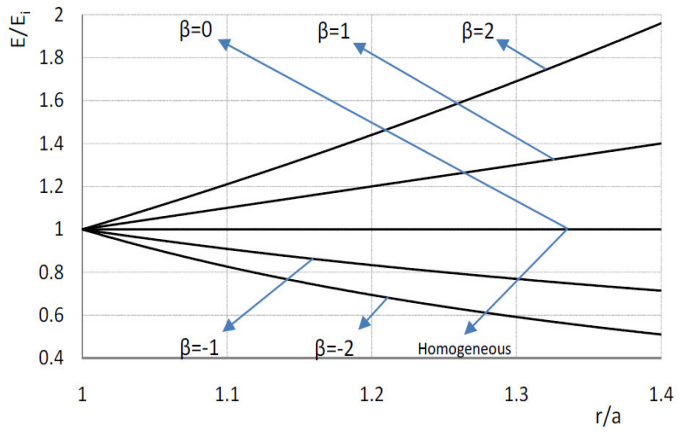

Figure 1. Distribution of modulus of elasticity.

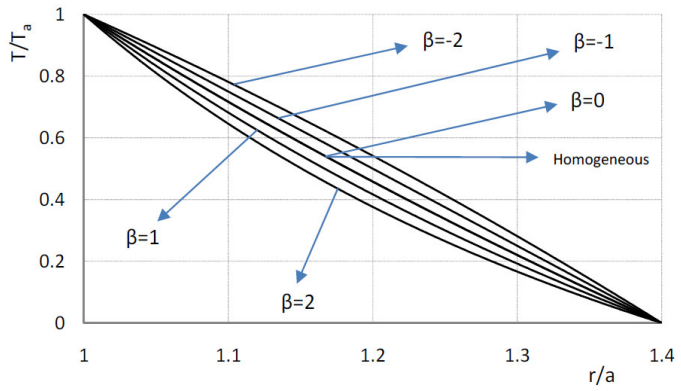

Figure 2. Distribution of radial temperature.

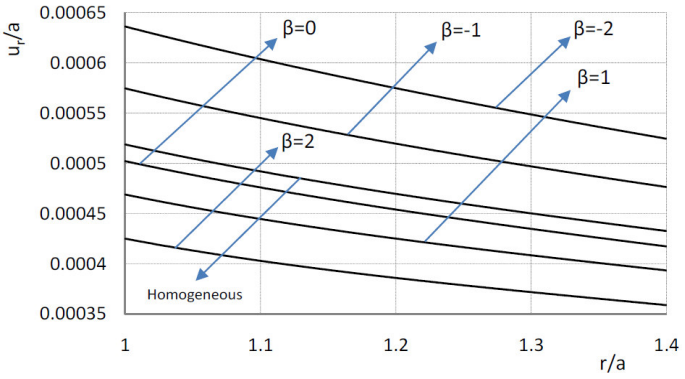

Figure 3. Distribution of radial displacement for plane strain condition ($\omega = 50 rad/\sec$).

β means increasing stiffness in the radial direction whereas a negative value of β results in a decrease in stiffness in the radial direction. Figure 2 shows that as β increases, the temperature decreases. Figures 3 and 4 show that for higher values of β, radial displacement

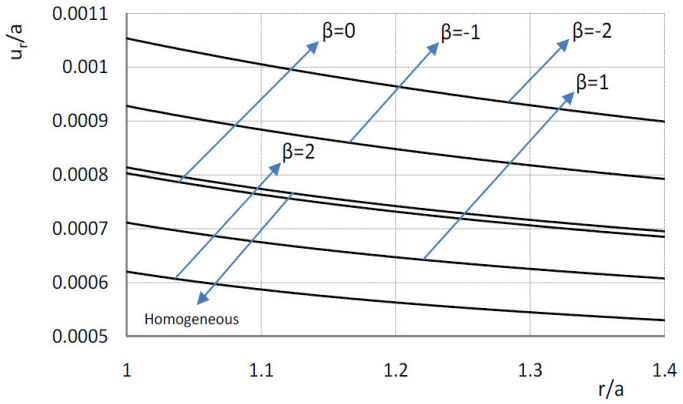

Figure 4. Distribution of radial displacement for plane stress condition ($\omega = 50 rad/\sec$).

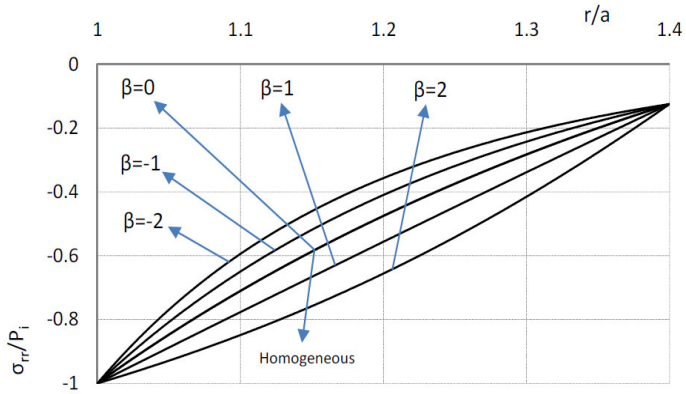

Figure 5. Distribution of radial stress for plane strain condition ($\omega = 50 rad/\sec$).

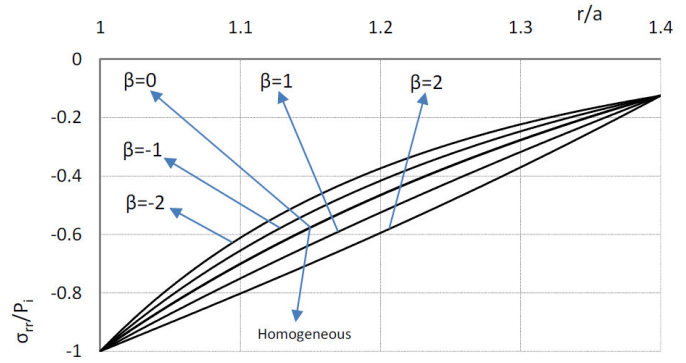

Figure 6. Distribution of radial stress for plane stress condition ($\omega = 50 rad/\sec$).

decreases. Besides, for similar values of β, the value of radial displacement is the highest for the plane stress condition and the lowest for the plane strain. Figures 5 - 8 show the distribution of radial and hoop stresses in the radial direction. As β increases, so does the magnitude

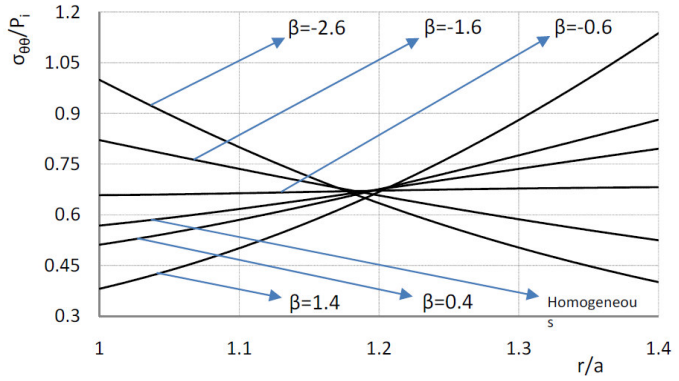

Figure 7. Distribution of hoop stress for plane strain condition ($\omega = 50 rad/\sec$).

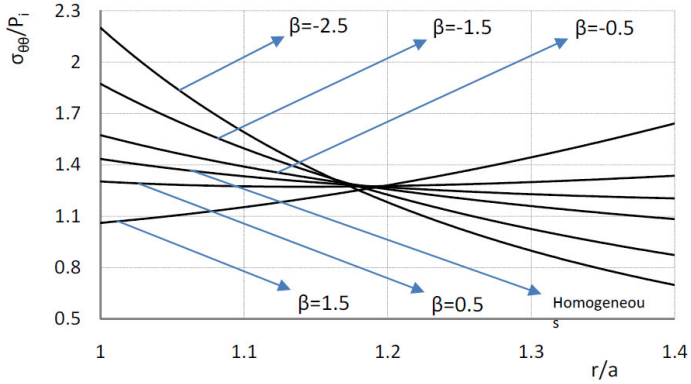

Figure 8. Distribution of hoop stress for plane stress condition ($\omega = 50 rad/\sec$).

of the radial stress. In the plane strain con-dition, for $\beta > -0.6$, the hoop stress increases as the radius increases whereas for $\beta < -0.6$ the hoop stress along the radius decreases. In the plane stress condition, for $\beta > 0.5$, the hoop stress increases as the radius increases whereas for $\beta < 0.5$ the hoop stress along the radius decreases. The curve associated with $\beta = -0.6$ and $\beta = 0.5$ for plane strain and plane stress conditions respectively, shows that the variation of hoop stress along the radial direction is minor and is almost uniform across the radius.

For the purpose of studying the pattern of stress distribution along the cylinder radius, in Figures 9 and 10, the von Mises' equivalent stress is plotted in the radial direction for the conditions of plane strain and plane stress. It must be noted that for $\beta = 2$, the equivalent stress remains almost uniform along the radius of the cylinder. Approximately, for $\beta > 2$, the von Mises' equivalent stress increases as the radius increases whereas for

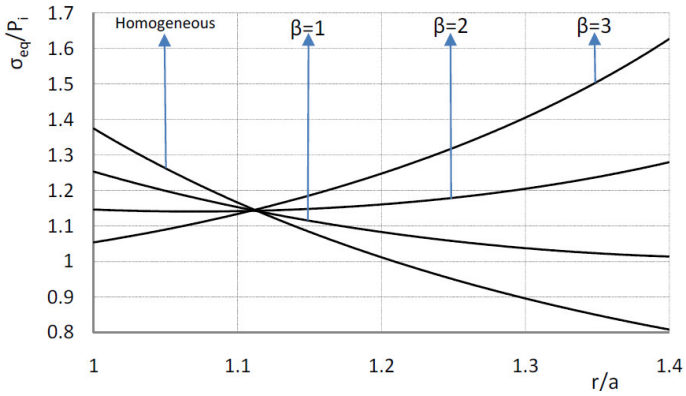

Figure 9. Distribution of equivalent stress for plane strain condition ($\omega = 50 rad/\sec$).

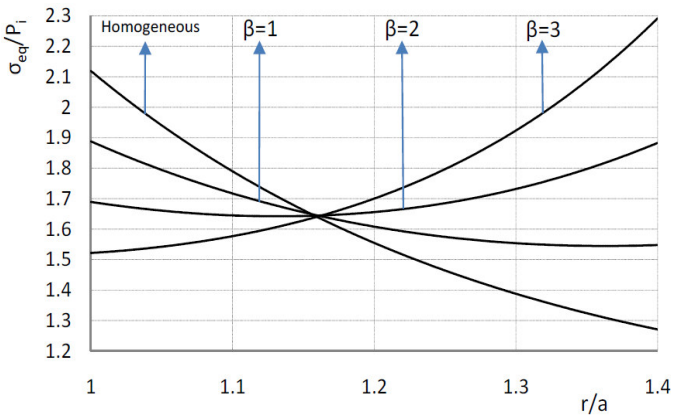

Figure 10. Distribution of equivalent stress for plane stress condition ($\omega = 50 rad/\sec$).

$\beta < 2$ it decreases. In almost all the figures, the homogeneous condition showed a behavior very similar to $\beta = 0$.

Example 2: In this example, the assumptions made in the previous case hold true, but $\beta = \mu = \eta = \xi = -1.5$, and the angular speed varies. In addition, ω ranges from $0\ rad/s$ to $300\ rad/s$.

For different values of ω, radial displacement, radial stresses, hoop stresses and the von Mises' equivalent stresses along the radial direction are plotted for plane strain and plane stress conditions in Figures 11 – 18. According to Figures 11 and 12, for higher values of ω, valent stress increases as the radius increases whereas for $\beta < 2$ it decreases. In almost all the figures, the homogeneous condition showed a behavior very similar to $\beta = 0$.

Example 2: In this example, the assumptions made in

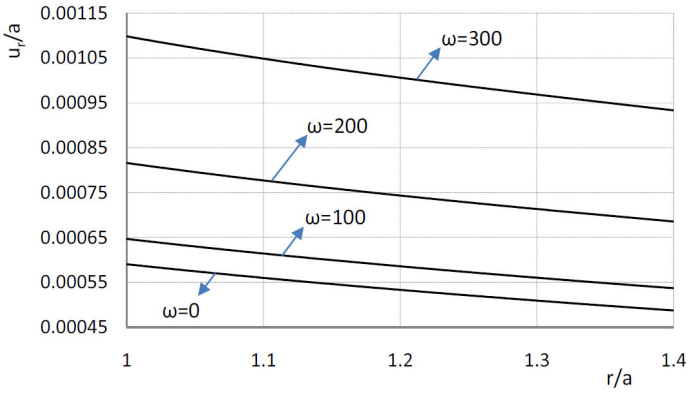

Figure 11. Distribution of radial displacement for plane strain condition ($\beta = \mu = \eta = \xi = -1.5$).

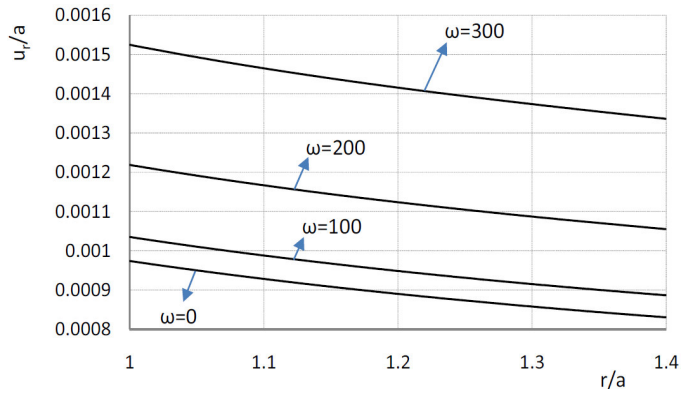

Figure 12. Distribution of radial displacement for plane stress condition ($\beta = \mu = \eta = \xi = -1.5$).

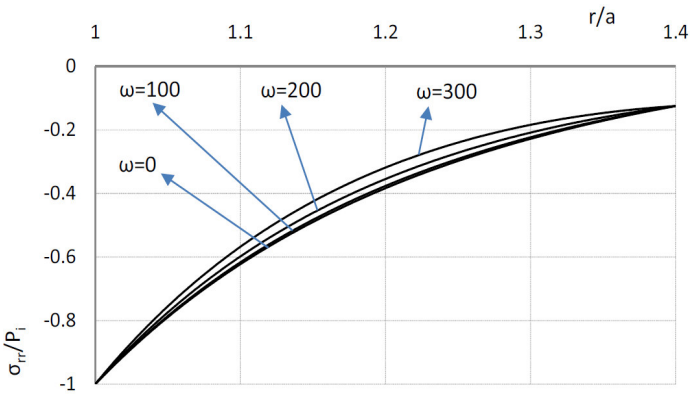

Figure 13. Distribution of radial stress for plane strain condition ($\beta = \mu = \eta = \xi = -1.5$).

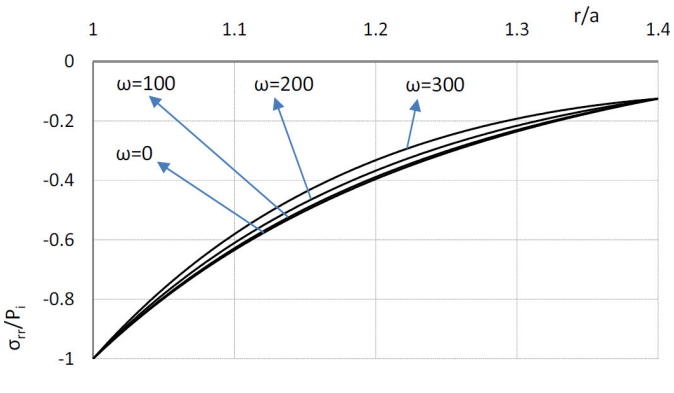

Figure 14. Distribution of radial stress for plane stress condition ($\beta = \mu = \eta = \xi = -1.5$).

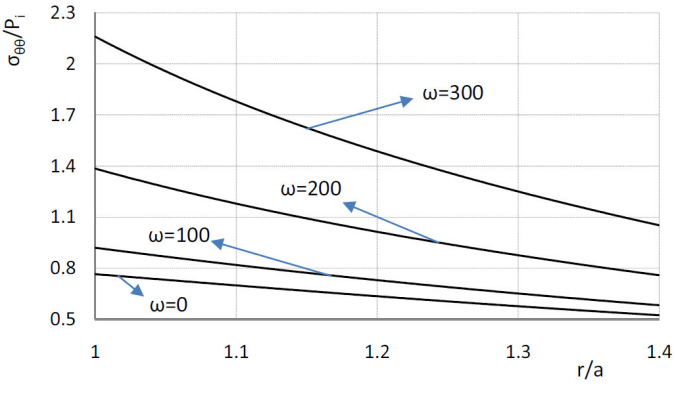

Figure 15. Distribution of hoop stress for plane strain condition ($\beta = \mu = \eta = \xi = -1.5$).

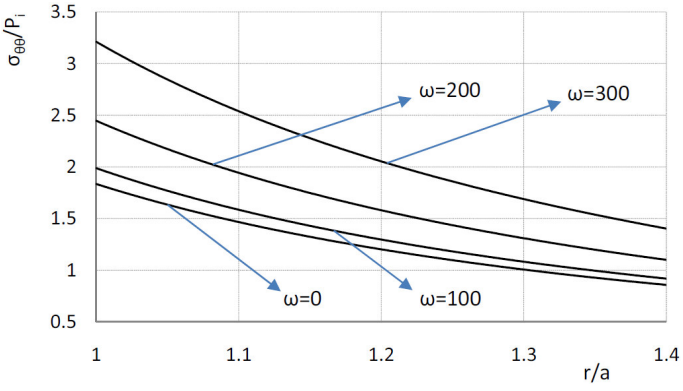

Figure 16. Distribution of hoop stress for plane stress condition ($\beta = \mu = \eta = \xi = -1.5$).

the previous case hold true, but $\beta = \mu = \eta = \xi = -1.5$, and the angular speed varies. In addition, ω ranges from $0\ rad/s$ to $300\ rad/s$.

For different values of ω, radial displacement, radial stresses, hoop stresses and the von Mises' equivalent stresses along the radial direction are plotted for plane strain and plane stress conditions in Figures 11 – 18.

According to Figures 11 and 12, for higher values of ω, radial displacement increases. Figures 13 – 14 show the

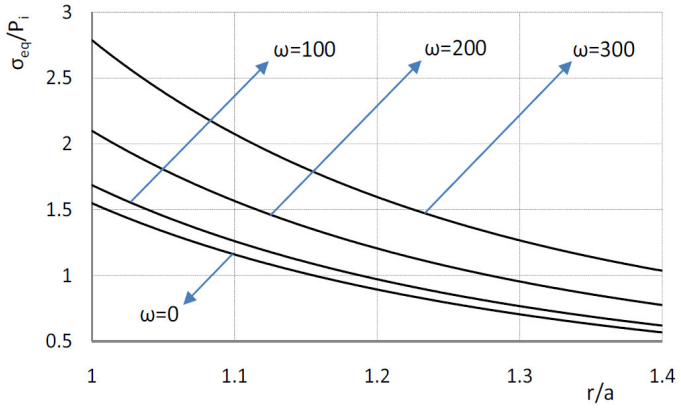

Figure 17. Distribution of equivalent stress for plane strain condition ($\beta = \mu = \eta = \xi = -1.5$).

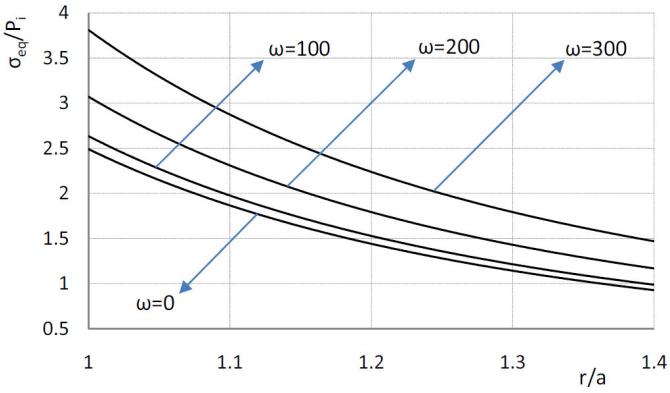

Figure 18. Distribution of equivalent stress for plane stress condition ($\beta = \mu = \eta = \xi = -1.5$).

distribution of radial stresses in the radial direction. The radial stress decreases as ω increases.

Figures 15 - 18 show the distribution of hoop stresses and equivalent stresses in the radial direction. The hoop and equivalent stress increase as ω increases. Besides, in all the Figures (11 - 18), for similar values of ω, the values of radial displacement, radial stresses, hoop stresses and equivalent stresses are highest for the plane stress condition but lowest for the plane strain. For a given ω, the same values decrease in radial direction.

Conclusion

It is apparent that closed form solutions to simplified versions of real engineering problems are important. In the present work, specifically, plane strain and plane stress, closed form solutions for the rotating FGM pressurized thick hollow cylinder under thermal load are derived and will be compared with those for the homogeneous ones. It is assumed that the material properties change as graded in the radial direction to a power law function. The values of μ, η and ξ are taken as coefficients of the values of β. To show the effect of in-homogeneity on the stress distributions, different values were considered for β and ω. In the first condition, β was considered to be constant and ω varying. In the second condition, this situation was reversed. The solution of the Navier equation yielded the mechanical and thermal stresses. Numerical results show that the in-homogeneous a useful parameter from a design point of view in that it can be tailored to specific applications to control the stress distributions. Thus, by selecting a proper value of β, it is possible for engineers to design rotating FGM pressurized thick hollow cylinder under a thermal load that can meet some special requirements. It is also possible to find an optimum value for the power law index such that the variation of stresses along the radial direction is minimized, yielding optimum use of material.

Nomenclature: A_1, A_2, A_{11} to A_{13}, A_1', A_2', B_1, to B_3, C_1 to C_5, C_1' to C_4', D_1 to D_6, D_1' to D_6' m_1 to m_5, n, Constants; a, inner radius of cylinder (m); b, outer radius of cylinder (m); E, modulus of elasticity (GPa); E^H, modulus of elasticity in homogeneous case (GPa); E_i, modulus of elasticity at the inner surface (GPa); h_a, heat transfer coefficients at the inner surface $W/(m^2.k)$; h_b, heat transfer coefficients at the outer surface $W/(m^2.k)$; k, thermal conductivity $W/(m.k)$; k^H, thermal conductivity in homogeneous case $W/(m.k)$; k_i, thermal conductivity at the inner surface $W/(m.k)$; P_i, internal pressure (MPa); P_o, external pressure (MPa); r, radius (m); $\bar{r}$, normalized radius; T, radial temperature (^0C); T^H, radial temperature in homogeneous case (^0C); T_a, inner temperatures of the surrounding media; T_b, outer temperatures of the surrounding media; u_r, radial displacement (m); u_r^H, radial displacement in homogeneous case (m); α, thermal conductivity $(/^o C)$; α^H, thermal conductivity in homogeneous case $(/^o C)$; α_i, thermal conductivity at the inner surface $(/^o C)$; β, inhomogeneity constant; η, inhomogeneity constant; θ, hoop +direction; μ, inhomogeneity constant; υ, Poisson's ratio; ξ, inhomogeneity constant; ρ, density (kg/m^3); ρ^H, density in homogeneous case (kg/m^3); ρ_i, density at the inner surface (kg/m^3); σ_{rr}, radial stress component (MPa);

$\sigma_{\theta\theta}$, hoop stress component (MPa).

REFERENCES

Argeso H, Eraslan AN (2008). On the use of temperature-dependent physical properties in thermomechanical calculations for solid and hollow cylinders. Int. J. Therm. Sci. 47: 136–146.

Chen YZ, Lin XY (2008). Elastic analysis for thick cylinders and spherical pressure vessels made of functionally graded materials. Comput. Mater. Sci. 44: 58–587.

Horgan CO, Chan AM (1999). The pressurized hollow cylinder or disk problem for functionally graded isotropic linearly elastic materials. J. Elast. 55: 43–59.

Jabbari M, Mohazzab AH, Bahtui A, Eslami MR (2007). Analytical solution for three-dimensional stresses in a short length FGM hollow cylinder. ZAMM. Z. Angew. Math. Mech. 87: 413-429.

Jabbari M, Sohrabpour S, Eslami, MR (2002). Mechanical and thermal stresses in a functionally graded hollow cylinder due to radially symmetric loads. Int. J. Press. Ves. Piping. 79: 493–497.

Liew KM, Kitipornchai S, Zhang XZ, Lim CW (2003). Analysis of the thermal stress behaviour of functionally graded hollow circular cylinders. Int. J. Solid. Struct. 40: 2355–2380.

Noda N (1991). Thermal stresses in materials with temperature-dependent properties. Appl. Mech. Rev. 44: 383–97.

Obata Y, Noda N (1994). Steady thermal stresses in a hollow circular cylinder and a hollow sphere of a functionally gradient material. J. Therm. Stress. 17: 471–487.

Ootao Y, Tanigawa Y, Nakamura T (1999). Optimization of material composition of FGM hollow circular cylinder under thermal loading: a neural network approach. Compos. Part B: Eng. 30: 415–422.

Pan E, Roy AK (2006). A simple plane-strain solution for functionally graded multilayered isotropic cylinders. Struct. Eng. Mech. 24: 727-740.

Rees DWA (2000). Mechanics of Solids and Structures. Imperial College Press. London.

Shao ZS (2005). Mechanical and thermal stresses of a functionally graded circular hollow cylinder with finite length. Int. J. Press. Ves. Piping. 82: 155–163.

Shao ZS, Ma GW (2008). Thermo-mechanical stresses in functionally graded circular hollow cylinder with linearly increasing boundary temperature. Compos. Struct. 83: 259–265.

Tanigawa Y (1995). Some basic thermoelastic problems for nonhomogeneous structural materials. Appl. Mech. Rev. 48: 287–300.

Tarn JQ, Wang YM (2004). End effects of heat conduction in circular cylinders of functionally graded materials and laminated composites. Int. J. Heat and Mass Transfer. 47: 5741–5747.

Timoshenko S, Goodier JN (1970). Theory of Elasticity. 3rd Ed. McGraw-Hill. New York.

Tutuncu N (2007). Stresses in thick-walled FGM cylinders with exponentially-varying properties. Eng. Struct. 29: 2032–2035.

Tutuncu, N, Ozturk M (2001). Exact solutions for stresses in functionally graded pressure vessels. Compos. Part B: Eng. 32: 683–686.

Ugural AC, Fenster SK (2003). Advanced Strength and Applied Elasticity, 4th Ed. Prentice-Hall. London.

You LH, Ou H, Li J (2007). Stress analysis of functionally graded thick-walled cylindrical vessels. AIAA J. 45: 2790–2798.

Zimmerman RW, Lutz MP (1999). Thermal stresses and thermal expansion in a uniformly heated functionally graded cylinder. J. Therm. Stress. 22: 177–188.